

# PhDay Físicas 2020



## Índice

[Supersaturated Ti implanted GaAs for photovoltaic and photodetector applications](#)

[One-Dimensional Moiré Superlattices and Flat Bands in Collapsed Chiral Carbon Nanotubes](#)

[Topological semimetals: robustness and tuning of the Fermi arcs](#)

[Polarización del vacío y colapso gravitatorio regular](#)

[Lumped Element Superconducting Resonators for Quantum Computing with Molecular Spin Qubits](#)

[Understanding the UV luminescence of zinc germanate: The role of native defects](#)

[Activation measurements of interest in protontherapy](#)

[Dictionary-based protoacoustic imaging for proton range verification](#)

[Wide companions to M and L subdwarfs with Gaia DR2 and the Virtual Observatory](#)

[Nonsingular black holes in Modified Gravity](#)

[The Gaia-ESO Survey: Calibrating the lithium-age relation with open clusters and associations](#)

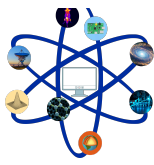
[Estados de gato robustos en sistemas de bosones controlados cinéticamente](#)

[Electromigration processes in the rapid synthesis of MoO<sub>3</sub> nanostructures](#)

[Climate-change-projection constraints from inaccurate estimates of the required depth of Land Surface Models](#)

[Dictionary Dose Reconstruction: A workflow for in-vivo dose verification in proton therapy](#)

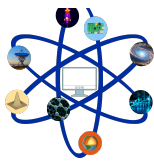
[Nuevos dispositivos eléctricos y magnéticos para aplicaciones en tecnología biomédica](#)



## 1. Supersaturated Ti implanted GaAs for photovoltaic and photodetector applications

Sari Algaidy

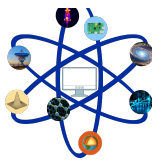
The evolution of the semiconductor industry requires the development of materials with improved properties. The formation of an IB (Intermediate Band) would allow the absorption of photons with energies below the bandgap. This would improve the efficiency of solar cells and open new possibilities for the fabrication of infrared detectors. GaAs is a strong candidate for this, due to the capability to improve GaAs based device performance and owing to its direct bandgap nature. One approach to form the intermediate band is the supersaturation of the semiconductor with deep level impurities. In this work, we analyse the supersaturation of GaAs with Ti by ion implantation followed by PLM (Pulsed Laser Melting) with concentrations to theoretically overcome the IB limit formation. The samples were implanted with titanium and melted using an ArF excimer laser. The crystallinity of the supersaturated layer was analysed by Raman spectroscopy and cross-sectional TEM (Transmission Electron Microscopy). The impurity concentration depth profile of the incorporated Ti was obtained by ToF-SIMS (Time of Flight – Secondary Ion Mass Spectroscopy). The processed samples also undergone electrical and opto-electrical measurements using van der Pauw set up, hall measurements and photoconductivity measurements.



## 2. One-Dimensional Moiré Superlattices and Flat Bands in Collapsed Chiral Carbon Nanotubes

Olga Arroyo Gascón

We demonstrate that one-dimensional moiré patterns, analogous to those found in twisted bilayer graphene, can arise in collapsed chiral carbon nanotubes. Resorting to a combination of approaches, namely, molecular dynamics to obtain the relaxed geometries and tight-binding calculations validated against ab initio modeling, we find that magic angle physics occur in collapsed carbon nanotubes. Velocity reduction, flat bands, and localization in AA regions with diminishing moiré angle are revealed, showing a magic angle close to  $1^\circ$ . From the spatial extension of the AA regions and the width of the flat bands, we estimate that many-body interactions in these systems are stronger than in twisted bilayer graphene. Chiral collapsed carbon nanotubes stand out as promising candidates to explore many-body effects and superconductivity in low dimensions, emerging as the one-dimensional analogues of twisted bilayer graphene.



## 3. Topological semimetals: robustness and tuning of the Fermi arcs

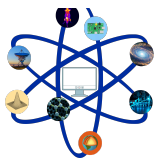
Yuriko Caterina Baba

Topological semimetals have attracted much interest in the last decade due to the promising new properties, especially thanks to their robust metallic surface states in 3D materials [1]. These surface states are called Fermi arcs and exist in open compact curves in the Brillouin zone. They are similar to the well-known 2D helical states of topological insulators. In Dirac semimetals, the linear dispersion of these states has the sign of their chirality. The effect of external perturbations such as electric fields or inversion-breaking terms enables the tuning of the surface states leading to non-trivial effects in transport properties. An electric field perpendicular to the surface generates a chiral dependent renormalization of the Fermi velocity in realistic low energy effective models [2]. The renormalization of the Fermi velocity have a direct impact on the electronic transport properties and the dependence on the chirality envisions chiral electronic devices. On the other hand, the breaking of inversion symmetry produces a spin-orbit splitting that become non-negligible in a carefully designed sample [3]. In a slab of topological semimetal, a substrate with heavy atoms should induce a strong and controllable Rashba spin orbit coupling at the surface that will affect the Fermi arcs. In this case, the coupling between chiralities opens new possibilities for spin-dependent transport phenomena in a two-terminal device. Finally, we study the effect of the impurities in an effective formalism by computing the averaged Green functions of a binary-disordered system. In this way, we aim to check the stability and robustness of the Fermi arcs and extend this approach to the Dirac and Weyl nodes.

[1] N. P. Armitage, E. J. Mele, and A. Vishwanath, *Rev. Mod. Phys.* 90, 015001(2018).

[2] Y. Baba, Á. Díaz-Fernández, E. Díaz, F. Domínguez-Adame, and R. Molina *Phys. Rev. B* 100, 165105 (2019).

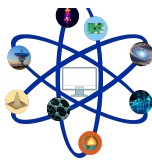
[3] Y. Baba, F. Domínguez-Adame, G. Platero and R. A. Molina, *arXiv:2009.14753* (2020).



## 4. Polarización del vacío y colapso gravitatorio regular

Valentín Boyanov Savov

El estado de vacío de un campo cuántico, a pesar de su nombre, puede tener un contenido energético. En particular, esto ocurre cuando el espaciotiempo en el que reside este campo es curvo. Este contenido energético a su vez es una fuente de curvatura adicional para la geometría espaciotemporal. La contribución de este efecto es despreciable para la mayoría de sistemas gravitatorios de interés astrofísico, con algunas excepciones importantes. Una de ellas es los espaciotiempos con agujero negro, donde el campo gravitatorio es tan fuerte que existen “zonas atrapadas” de las que no puede escapar ni siquiera la luz. El presente trabajo estudia el efecto que tienen estas regiones del espaciotiempo sobre el vacío cuántico, y el efecto que éste tiene a su vez sobre la evolución del espaciotiempo.



## 5. Lumped Element Superconducting Resonators for Quantum Computing with Molecular Spin Qubits

Marina Calero de Ory

Hybrid structures based on chemically engineered magnetic molecules spins strongly coupled to superconducting resonators are promising candidates for large-scale quantum processors, as they offer reproducibility and long coherence times [1]. Superconducting resonators exhibit low losses, critical for achieving strong coupling with spin systems. In this work, we will focus on the development of superconducting lumped element resonators (LERs). Each LER consists of a series inductance-capacitance circuit, which allows large freedom of design, coupled in parallel to a single transmission line [2]. The magnetic coupling with the spin system can be optimized by tuning key parameters, such as the resonator impedance, geometry or quality factor [3]. Furthermore, LERs are intrinsically multiplexable on-chip, permitting the simultaneous readout of several qubits. We will present the design, using microwave electromagnetic simulations to obtain the magnetic field distribution, fabrication and low temperature characterization of superconducting LERs. We have focused on addressing two different limits: coupling with large spin ensembles (as free-radical DPPH, Yb-Trensals or VO-Porphyrins, which could be used as qudits thanks to the electronuclear spin states [4]) and coupling with isolated spins (for which low impedance LERs offer an enhancement of the coupling to each spin thanks to a strong confinement of the magnetic field [5]).

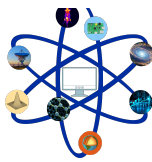
[1] M. Jenkins et al., Dalton Tran. 45, 16682 (2016).

[2] S. Doyle et al., J. Low Temp. Phys. 151, 530 (2008).

[3] S. Weichselbaumer et al., Phys. Rev. Applied 12, 024021 (2019).

[4] A. Urtizberea et al., Materials Horizons, 7, 885 (2020).

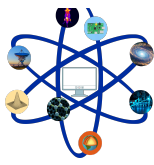
[5] L. McKenzie-Sell et al., Physical Review B, 99, 140414 (2019).



## 6. Understanding the UV luminescence of zinc germanate: The role of native defects

Jaime Dolado Fernández

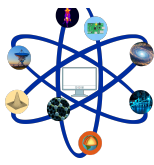
Achieving efficient and stable ultraviolet emission is a challenging goal in optoelectronic devices. Herein, we investigate the UV luminescence of zinc germanate  $\text{Zn}_2\text{GeO}_4$  microwires by means of photoluminescence measurements as a function of temperature and excitation conditions. The emitted UV light is composed of two bands (a broad one and a narrow one) associated with the native defects structure. In addition, with the aid of density functional theory (DFT) calculations, the energy positions of the electronic levels related to native defects in  $\text{Zn}_2\text{GeO}_4$  have been calculated. In particular, our results support that zinc interstitials are the responsible for the narrow UV band, which is, in turn, split into two components with different temperature dependence behaviour. The origin of the two components is explained on the basis of the particular location of Zn in the lattice and agrees with DFT calculations. Furthermore, a kinetic luminescence model is proposed to ascertain the temperature evolution of this UV emission. These results pave the way to exploit defect engineering in achieving functional optoelectronic devices to operate in the UV region.



## 7. Activation measurements of interest in protontherapy

Andrea Espinosa Rodríguez

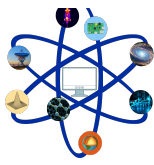
Full exploitation of the therapeutic potential of protontherapy is still prevented by uncertainties in the determination of the proton range within the patient's body. Several methods have been proposed to verify the proton range in-vivo by measuring the secondary activity (either PET or prompt-gamma) induced by proton fields. However, none of the presented solutions has yet reached clinical maturity, due to low activity counts and different spatial distributions of dose and proton-induced activity profiles. The quality of verification images can be largely improved by the use of contrast agents that provide an increased induced radioactivity near the Bragg-peak region. Iodine is a contrast agent already approved for a number of medical applications. It presents a promising proton reaction channel producing the metastable isomer  $^{127m}\text{Xe}$ , with a half-life of 69.2(9) s, which is a perfect radioisotope for online range verification. However, cross section production for this reaction is not adequately measured down to low proton energies relevant to the Bragg peak. We have put in place a specific set-up consisting of two pairs of collinear opposed  $\text{LaBr}_3$  detectors and a fully digital acquisition system, and performed irradiations in the low energy (2-10 MeV) range in the microbeam line at Center for Micro Analysis of Materials (Madrid, Spain). We report on a new measurement of  $^{127}\text{I}(p,n)^{127m}\text{Xe}$  reaction cross section down to 4.5 MeV by the activation technique. The accuracy of the measured cross sections is better than 30%, and the observed values are in agreement with theoretical calculations using the default parameters of the TALYS code. We have observed significant activity for proton energies above 3.75 MeV, corresponding to a range-in-water of less than 0.25 mm. Our results support the viability of  $^{127}\text{I}$  as a contrast agent for proton radiotherapy.



## 8. Dictionary-based protoacoustic imaging for proton range verification

Clara Freijo Escudero

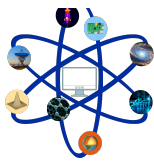
Proton radiotherapy employs proton beams for cancer treatment. This technique has the potential to provide state-of-the-art dose conformality in the tumor area, since protons have a limited range and deposit most of their energy at the end of their path, in the so-called Bragg peak region. Therefore, the extra dose that healthy tissues usually received during conventional photon radiotherapy can be reduced. However, uncertainties in the exact location of the proton Bragg peak prevent this technique from achieving full clinical potential. In this context, in vivo verification of the range of protons in patients is key to reduce uncertainty margins. One of the methods proposed for proton range verification is protoacoustics. This technique employs acoustic pressure waves generated by proton energy deposition, due to a physical process known as radio-induced thermoacoustic effect, to reconstruct the dose distribution map of protons in the patient. Nevertheless, dose image reconstruction implies a high computational cost which makes difficult to implement this technique in real time during treatment. In this work, we propose to use the a priori knowledge of the shape of the proton dose distribution to create a dictionary with the expected ultrasonic signals at predetermined detector locations. Using this dictionary, the reconstruction of the dose deposited is performed by matching pre-calculated dictionary acoustic signals with data acquired online during treatment. This system is especially suitable to detect treatment delivery errors. The dictionary-based proton range verification method was evaluated for a prostate cancer patient. We studied its ability to detect range variations caused by anatomical variations, patient position misalignment and errors in CT Hounsfield Units conversion to relative stopping power. Our results show that the dictionary-based protoacoustic method was able to identify the changes in range originated by all the alterations introduced, with an average accuracy of 1.1 mm. This procedure could be used for in vivo verification, since the in-house developed algorithm takes approximately 100 ms to identify the most probable Bragg peak position.



## 9. Wide companions to M and L subdwarfs with Gaia DR2 and the Virtual Observatory

Francisco Javier González Payo

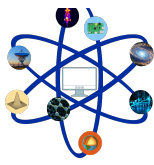
We performed a search for common proper motion companions to a sample of 219 spectroscopically confirmed M and L subdwarfs using Virtual Observatory tools, the Gaia DR2 catalogue and large-scale public photometric and astrometric surveys. After compiling some data from Gaia DR2 and estimating other ones if not available, we present six candidate systems with M primaries and projected physical separations between 0.007 and 2.6 pc. We found two M+M systems, one confirmed spectroscopically as metal-poor, and one with solar metallicity. We also identified four M+L wide binary systems (just one M+L extreme subdwarf system has been reported to date by Zhang et al. 2019, 2018MNRAS.479.1383Z). None of the non-confirmed five systems can be discarded based on current astrometry and photometry, so they require spectroscopy follow-up. The binary fraction in our sample is of 1.2% among our sample of M subdwarfs with separations between 0.007 and 2.6 pc. Binariness fraction for M and L extreme subdwarfs of 1.6%, and not found any ultra subdwarf as wide secondary, implying a multiplicity below 1%.



## 10. Nonsingular black holes in Modified Gravity

Mercè Guerrero Román

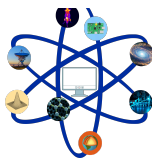
Static, spherically symmetric black holes coupled to two different modified theories of gravity are studied. Such theories are the quadratic  $f(R)$  model and Eddington-inspired Born-Infeld gravity, both formulated in metric-affine spaces, where metric and affine connection are independent fields. For each family of solutions, we characterize the modifications in the innermost region, finding that some subclasses are geodesically complete. The singularity regularization is achieved under two different mechanisms: either the boundary of the manifold is pushed to an infinite affine distance, not being able to be reached in finite time by any geodesic, or the presence of a wormhole structure allows for the smooth extension of all geodesics overcoming the maximum of the potential barrier.



## **11. The Gaia-ESO Survey: Calibrating the lithium-age relation with open clusters and associations**

**Marta Lúthien Gutiérrez Albarrán**

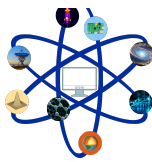
The large number of stars observed within the Gaia-ESO survey (GES) for many open clusters and associations can be used to calibrate the lithium-age relation and its dependence with other parameters. This relation will ultimately allow us to infer the ages of GES field stars and identify their potential membership to young associations and stellar kinematic groups. In the present work we performed a thorough analysis of membership and Li abundance of 20 clusters observed in GES (iDR4), ranging in age from young clusters and associations, to intermediate-age and old open clusters, to conduct a comparative study. All this allowed us to characterize the properties of the members of these clusters, as well as identify a series of field contaminant stars, both lithium-rich giants and non-giant outliers.



## 12. Estados de gato robustos en sistemas de bosones controlados cinéticamente

Jesús Mateos Maroto

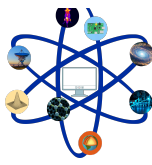
Se investiga el comportamiento del modelo de Bose-Hubbard unidimensional cuyo término cinético se hace oscilar con promedio temporal nulo. Para un valor crítico del "driving", el sistema pasa de un aislante de Mott a un superfluido formado por una superposición tipo gato de dos cuasi-condensados con momentos opuestos y no nulos. Se analiza la robustez de este estado fundamental poco convencional frente a variaciones de varios parámetros del sistema. En particular se estudia el efecto de la forma y el protocolo de encendido de la señal del "driving". El conocimiento de la sensibilidad del sistema a variaciones de estos parámetros permite estimar la robustez de este exótico comportamiento físico.



## 13. Electromigration processes in the rapid synthesis of MoO<sub>3</sub> nanostructures

Beatriz Rodríguez Fernández

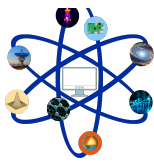
Study of the rapid synthesis of MoO<sub>3</sub> nanostructures from assisted electromigration processes through an external electric field in a molybdenum metallic wire. This technique introduces a rapid way for the synthesis of Van der Waals materials, which have multiple properties and very promising future applications. The results show that when a maximum current of 5A, for a time between a few seconds and a minute, causes a heating of the Mo wire around (450-500) C, giving rise to a high density of molybdenum oxide nanostructures mainly in the central part of the wire. The measurements of Raman spectroscopy, X-ray diffraction (XRD) and energy dispersion spectroscopy (EDS) performed in a scanning electron microscope reveal that the grown nanostructures are basically MoO<sub>3</sub> in orthorhombic phase. The growth mechanisms are discussed in terms of electromigration and local oxidation processes on the surface of the wire. To study in detail the electromigration processes of charge during growth, external electric fields have been applied perfectly oriented parallel and perpendicular to the axis of the Mo wire. These electric fields have been observed to alter the normal growth of nanostructures, because under certain orientations they can inhibit electromigration processes.



## 14. Climate-change-projection constraints from inaccurate estimates of the required depth of Land Surface Models

Norman Steinert

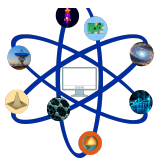
The representation of the ground thermal and hydrological state in climate models is crucial for a realistic simulation of subsurface processes and the coupling between the atmo-, lito- and biosphere. There is an inaccurate simulation of ground thermodynamics in state-of-the-art climate models due to too shallow soil models. The energy propagation and spatio-temporal variability of temperatures are distorted, which impedes the simulation of land-air interaction and subsurface phenomena. Therefore, we introduce a deeper soil in climate projections of the 21st century. The impacts of a deeper soil are 1) changes in the thermal state of up to 2K regionally, 2) significant changes in the ground energy storage of 5-10 times the magnitude, 3) implications for permafrost evolution, which translate to uncertainty in carbon-release to the atmosphere. However, more complex climate models come with an increase in computational effort. In order to find the optimal soil depth for future climate projections, we compare the error of simulations with a deep and shallow soil to the classic analytical case by adjusting it to better fit our projected temperature signal and obtain a more precise estimate of the required soil depth by 50% and a reduction in the error by a factor of 3. This allows for a more effective use of computational resources along with a more realistic simulation of the future climate as a basis for decision-makers to drive the agreement on future carbon emission targets.



## **15. Dictionary Dose Reconstruction: A workflow for in-vivo dose verification in proton therapy**

Víctor Valladolid Onecha

La protonterapia es una técnica de radioterapia que usa protones como partículas ionizantes para irradiar tumores. La principal ventaja de esta técnica con respecto a las tradicionales es la forma en la que los protones depositan la energía, que se caracteriza por concentrar la energía al final el rango del protón generando un pico de dosis muy bien definido que permite conformar la dosis de forma mucho más precisa que en radioterapia con fotones. El problema que tiene esta técnica es que es necesaria una precisión en el cálculo del rango del protón no existente hoy en día para poder usarse en un ámbito clínico más extenso y de forma más eficaz. Una de las técnicas más desarrolladas para la verificación de rango del protón es el usar un scanner PET para medir los isótopos beta+ generados por los protones, y calcular la dosis a partir de cómo se han generado estos isótopos. El problema es que este proceso de pasar de activación PET a dosis no es sencillo y actualmente no existe ningún método capaz de realizar este proceso de forma rápida y precisa. Nuestro trabajo consiste en el desarrollo de un proceso de trabajo para calcular la dosis depositada, con una precisión milimétrica y en tiempo real durante un tratamiento de protonterapia, capaz de identificar desviaciones con respecto a lo planeado. Para este fin hemos desarrollado un método de reconstrucción de Activación PET capaz de reconstruir, a partir de una base de datos precalculada, cualquier activación en la zona que se pretenda estudiar. La base de datos está compuesta por muchos pares de contribuciones de activación y su dosis correspondiente, de forma que buscando la combinación de activaciones que mejor representa la imagen PET reconstruimos también la dosis depositada en el paciente.



## **16. Nuevos dispositivos eléctricos y magnéticos para aplicaciones en tecnología biomédica**

**Arturo Vera García**

Mi tesis doctoral se enmarca dentro del proyecto ByAxon, dedicado al desarrollo de una nueva interfaz neuronal basada en materiales nanotecnológicos. El fin último de esta interfaz es restaurar la transmisión de señales eléctricas en un paciente con la médula espinal lesionada. Para ello se pretende fabricar un implante activo que pueda funcionar directamente a nivel de la médula espinal, actuando como un bypass local activo. Los enfoques actuales de interfaz neuronal se basan en la detección de potenciales eléctricos a nivel cerebral y / o en la activación de la estimulación eléctrica funcional (FES) a través de electrodos a niveles musculares o de espina dorsal. Sin embargo, estos enfoques presentan inconvenientes, como la gran cantidad de cables y electrodos que requieren y, especialmente, la falta de retroalimentación sensorial. Los últimos dispositivos de detección sin contacto (magneto encefalografía) detectan pulsos de campo magnético generados por potenciales en el cerebro, pero requieren temperaturas criogénicas y, por lo tanto, no son portátiles. Por este motivo ByAxon usará sensores magnéticos para detectar la actividad neuronal en la parte no dañada y electrodos para excitar la parte afectada por la lesión. En este trabajo presentaré los avances llevados a cabo por el grupo en la detección de señales neuronales mediante sensores magnéticos utilizando sensores basados en magneto resistencia túnel. Dichos campos poseen típicamente una amplitud de entorno 10nT, por lo que su detección supone un desafío tanto a nivel de desarrollo de sensores como de la electrónica que permita discriminar unas señales tan pequeñas. En particular, presentaré el prototipo desarrollado que permite suprimir el ruido electromagnético ambiente que impediría la detección de señales neuronales magnéticas. Dicho prototipo ha sido probado en tejido neural cultivado (ex-vivo) y ha permitido obtener medidas de la actividad neural en condiciones de laboratorio y sin apantallamiento magnético. Los resultados obtenidos representan el primer paso hacia el desarrollo de un prototipo final implantable en la médula espinal.